Journal of Peptide Science, Vol. 1, 45–57 (1995)

Synthesis and Conformational Studies of Peptides Containing TOAC, a Spin-labelled $C^{\alpha,\alpha}$-disubstituted Glycine

CLAUDIO TONIOLO[1], EZIO VALENTE[1], FERNANDO FORMAGGIO[1], MARCO CRISMA[1], GIUSEPPE PILLONI[2], CARLO CORVAJA[3], ANTONIO TOFFOLETTI[3], GARY V. MARTINEZ[4], M. PAUL HANSON[4], GLENN L. MILLHAUSER[4], CLIFFORD GEORGE[5] and JUDITH L. FLIPPEN-ANDERSON[5]

[1] Biopolymer Research Centre, CNR, Department of Organic Chemistry, University of Padova, Padova, Italy
[2] Department of Inorganic, Metallorganic and Analytical Chemistry, University of Padova, Padova, Italy
[3] Department of Physical Chemistry, University of Padova, Padova, Italy
[4] Department of Chemistry and Biochemistry, University of California, Santa Cruz, California, USA
[5] Laboratory for the Structure of Matter, Naval Research Laboratory, Washington, DC, USA

Received 30 March 1994
Accepted 3 May 1994

Abstract: A variety of host L-alanine homo-peptides (to the pentamer) containing one or two spin-labelled TOAC (2,2,6,6-tetramethylpiperidine-1-oxyl-4-amino-4-carboxylic acid) residues were synthesized by solution methods and fully characterized. The conformational features of the terminally blocked, doubly spin-labelled –TOAC–$(Ala)_2$–TOAC–Ala– pentapeptide were examined in the crystal state by X-ray diffraction and in solution using a combination of techniques (Fourier transform infrared, circular dichroism, cyclic voltammetry and electron spin resonance) in comparison with singly labelled shorter peptides. The 3_{10}-helical structure of the pentapeptide, promoted by the two $C^{\alpha,\alpha}$-disubstituted glycines under favourable experimental conditions, allows an interaction to take place between the two nitroxide TOAC side chains spaced by one turn of the helix. Taken together, these results suggest that TOAC is an excellent probe for exploring bends and helices in doubly labelled peptides.

Keywords: β-bend; 3_{10}-helix; peptide conformational analysis; spin-labelled amino acid; TOAC peptides

Abbreviations

TOAC, 2,2,6,6-tetramethylpiperidine-1-oxyl-4-amino-4-carboxylic acid; Ac_6c, 1-aminocyclohexane-1-carboxylic acid; Aib, α-aminoisobutyric acid or $C^{\alpha,\alpha}$-dimethylglycine; Ac, acetyl; *p*BrBz, *para*-bromobenzoyl; NHMe, methylamino; NH*t*Bu, *tert*-butylamino; TFE, 2,2,2-trifluoroethanol; HFIP, 1,1,1,3,3,3-hexafluoroisopropanol; MD, molecular dynamics.

INTRODUCTION

The great structural versatility of the family of $C^{\alpha,\alpha}$-disubstituted glycines has recently emerged as a focal point in the field of bioactive peptide mimicry [1, 2]. More specifically, the strongly preferred conformations (β-bends and 3_{10}-/α-helices) theoretically postulated and experimentally found both in the crystal state and in solution for

* Address for correspondence: Prof. Claudio Toniolo, Department of Organic Chemistry, University of Padova, via Marzolo 1, 35131 Padova, Italy.

CCC 1075-2617/95/010045-13

the cycloaliphatic Ac_6c residue closely parallel those of the extensively investigated prototype Aib [3–5].

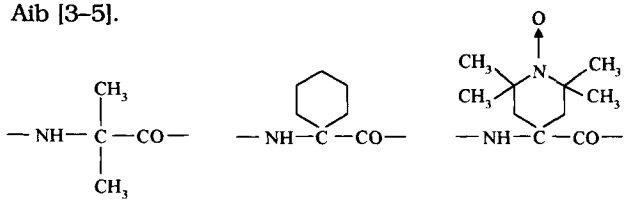

Aib Ac_6c TOAC

As a logical extension of the structural investigations of Ac_6c, our efforts recently focused on TOAC, a saturated heterocyclic analogue containing a stable paramagnetic label. A favourable property of TOAC over other spin-labelled amino acids is that rotation about side-chain bonds is hampered by incorporation of the nitroxide nitrogen and C^{α}, C^{β} and C^{γ} atoms into a cyclic moiety. In general, amino acids with nitroxide modified side chains play an important role in providing useful electron spin resonance (ESR) information on the preferred conformations of peptide molecules [6, 7] and on their interactions with macromolecules and biological membranes [8]. However, they might also be exploited as potentially valuable probes in the study of organic materials showing ferromagnetic properties [9] and of redox processes [10]. In spite of all these possible applications, we were rather surprised to find that TOAC, although introduced in peptide chemistry more than a decade ago [11], has been employed so far only in a very limited number of studies [12–16].

In this paper we describe the synthesis and characterization of a number of TOAC derivatives and L-alanine-based peptides (to the pentamer level) in which one or two TOAC residues are incorporated at different positions of the sequence. An extensive conformational analysis was performed in the crystal state (by X-ray diffraction) and in solution (by Fourier transform infrared spectroscopy (FTIR), circular dichroism (CD), cyclic voltammetry and ESR) on a doubly labelled pentapeptide with the sequence -TOAC-(Ala)$_2$-TOAC-Ala-. The results obtained, in comparison with those of the singly labelled, shorter peptides, favour the conclusion that the pentapeptide is folded in the right-handed 3_{10}-helical conformation under structure-supporting experimental conditions. A concomitant interaction is seen between the two nitroxide side chains aligned in the structure one on the top of the other after one turn of the helix.

MATERIALS AND METHODS

Synthesis and Characterization of Peptides

Melting points were determined using a Leitz (Wetzlar, Germany) model Laborlux 12 apparatus and are not corrected. Optical rotations were measured using a Perkin-Elmer (Norwalk, CT) model 241 polarimeter equipped with a Haake (Karlsruhe, Germany) model D thermostat. Thin-layer chromatography was performed on Merck (Darmstadt, Germany) Kieselgel $60F_{254}$ precoated plates using the following solvent systems: 1 ($CHCl_3$–EtOH, 9:1), 2 (Bu^nOH–AcOH–H_2O, 3:1:1); 3 (toluene–EtOH 7:1). The chromatograms were examined by UV fluorescence or developed by chlorine–starch–potassium iodide or ninhydrin chromatic reaction as appropriate. All the compounds were obtained in a chromatographically homogeneous state. Amino acid analyses of the Ala/TOAC peptides were not performed as TOAC is unstable under the acidic conditions required for hydrolysis of the –CONH–, –OCONH– and –COO– bonds.

X-ray Diffraction

Crystals (0.72 × 0.16 × 0.07 mm) of *p*BrBz-TOAC-(L-Ala)$_2$-TOAC-L-Ala-NH*t*Bu (hemihydrate) were grown by slow evaporation from a methanol solution. The intensities of the diffracted beam were measured at room temperature on a four-circle automated diffractometer with CuKα radiation (λ = 1.5418 Å) and a graphite monochromator in the incident beam. Three reflections that were used as standards were monitored every 97 measurements and remained constant within 3.5% during the data collection. A 1.2° scan with a variable scan speed from 7 to 30°/min, depending on the intensity of a reflection, was used in a $\theta/2\theta$ mode with $2\theta_{max}$ = 112° (resolution = 0.9 Å). The data were corrected for Lorentz and polarization effects and an empirical absorption was applied (min/max transmission factors 0.382/0.741). The number of independent data collected was 3189 (R_{int} = 0.0201) with 2531 data observed with $I > 2\sigma(I)$, crystal system monoclinic, space group $P2_1$, a = 11.451(2) Å, b = 18.932(4) Å, c = 11.741(2) Å, β = 112.15(2) °, Z = 2. The calculated density was 1.233 g/cm^3, based on a molecular weight of 874.92 a.m.u. for $C_{40}H_{65}N_8O_8Br \cdot 1/2H_2O$, two formula units per cell, and cell volume V = 2357.5(8) Å^3. The structure was

solved by direct phase determination using program SHELX 86 [17]. Full-matrix anisotropic least-squares refinement, using program SHELXS 93 [18] on F^2 values, using the full set of data, was performed on the non-hydrogen atoms before hydrogen atoms were added in idealized positions and allowed to ride with the C, N and O atoms to which each was bonded. The number of parameters refined was 520 with a data to parameter ratio of approximately 6:1. The final traditional R factor was 9.23% for 2531 data observed $I > 2\sigma(I)$ and 10.94% for all the data. Complete lists of bond lengths, bond angles and torsion angles, and the final positional parameters for all non-hydrogen atoms along with their thermal factors have been deposited and are available from the Cambridge Crystallographic Data Centre (Cambridge, UK).

IR Absorption

The solid-state IR absorption spectra (KBr disk technique) were recorded with a Perkin-Elmer model 580B spectrophotometer equipped with a Perkin-Elmer model 3600 data station. The solution spectra were obtained using a Perkin-Elmer model 1720X FTIR spectrophotometer, nitrogen-flushed, equipped with a sample-shuttle device, at 2 cm^{-1} nominal resolution, averaging 100 scans. Solvent (baseline) spectra were recorded under the same conditions. Cells with path lengths of 0.1, 1.0 and 10 mm (with CaF_2 windows) were used. Spectrograde deuterochloroform (99.8% *d*) was purchased from Fluka (Buchs, Switzerland).

UV–VIS Absorption and Circular Dichroism

The UV–VIS spectra were obtained using a Perkin-Elmer model Lambda 5 spectrophotometer. A quartz cell (Hellma, Müllheim, Germany) of 10 mm path length was used. The CD spectra were recorded on a JASCO (Tokyo, Japan) model J-600 spectropolarimeter equipped with a Haake thermostat. Cylindrical fused quartz cells of 10 and 1 mm path lengths were employed. The values are expressed in terms of $[\theta]_M$, the total molar ellipticity (deg cm^2 $dmol^{-1}$). MeOH (Riedel-de-Häen, Seelze, Germany), EtOH (C. Erba, Rodano, Milan, Italy), TFE, HFIP and $CHCl_3$ (Fluka) and DMSO (Merck) were used as solvents.

Cyclic Voltammetry

All experiments were performed on anhydrous deoxygenated EtOH solutions with 0.2 M sodium perchlorate as the supporting electrolyte, using a conventional three-electrode liquid-jacketed cell. Cyclic voltammetry measurements were performed with an Amel (Milan, Italy) model 551 potentiostat modulated by an Amel 566 function generator. The recording device was an Amel model 863 *X–Y* recorder. The working electrode was a planar platinum microelectrode (*ca.* 0.3 mm^2) surrounded by a platinum spiral counter electrode. A silver/0.1 M silver perchlorate in acetonitrile, separated from the test solution by 0.2 M sodium perchlorate in EtOH solution sandwiched between two fritted disks, was used as the reference electrode. Compensation for *iR* drop was achieved by positive feedback. Ferrocene (Aldrich, Milwaukee, WI) was added at the end of each experiment as the internal reference. All potentials are referred to the ferrocenium/ferrocene couple (E° = +0.068 V relative to the actual Ag/$AgClO_4$ reference electrode).

Electron Spin Resonance Spectroscopy

X-band continuous wave experiments were carried out using a Bruker ESP 380 spectrometer. A TE_{102} cavity was used for high-concentration samples (0.3–3 mM peptide) and a high-sensitivity dielectric resonator was used for samples with lower concentrations (0.03–0.3 mM peptide). Dissolved oxygen was removed by bubbling nitrogen gas for several minutes. Samples contained 30 µl of peptide solution and were sealed in glass microcapillary tubes. Temperature control was accomplished with a Bruker variable temperature accessory. All solutions were subjected to high temperature to determine whether broadening was due to peptide aggregation. Only TFE showed evidence of peptide aggregation after dissolution and this aggregation was eliminated by cycling the temperature up to 343 K and then back down to 296 K. Spectra were gathered over a 80 gauss width; however, 200 gauss scans were performed on all samples to check for biradical singlet transitions. Quantitative spin integration, using a 1.0 mM TEMPO standard, was performed on each sample. Collection parameters included a mod. amp. of 0.4 gauss or less at a frequency of 100 kHz.

RESULTS

Synthesis of TOAC, TOAC Derivatives and Ala/TOAC Peptides

The free amino acid was prepared from the corresponding hydantoin by alkaline hydrolysis with barium hydroxide according to published procedures [13, 15, 19]. The hydantoin, in turn, was synthesized from 2,2,6,6-tetramethyl-4-oxo-piperidine-1-oxyl by treatment with ammonium carbonate and sodium cyanide [13, 19]. The Fmoc [16], Z [15], Boc [11, 12, 15] and *p*BrBz N^{α}-protected derivatives were obtained by reacting H-TOAC-OH with the pertinent *N*-hydroxysuccinimido derivatives. The 5(4*H*)-oxazolone from *p*BrBz-TOAC-OH was synthesized by reacting the free amino acid with an excess of *para*-bromobenzoylchloride in anhydrous pyridine. The symmetrical anhydride from Z-TOAC-OH and the 5(4*H*)-oxazolones from Z-, Fmoc- and Boc-TOAC-OH were prepared by dehydration of the corresponding N^{α}-protected amino acid with *N*-ethyl, *N'*-(3-dimethylaminopropyl)-carbodiimide. *Inter alia*, Fmoc-TOAC-OH and the 5(4*H*)-oxazolones from Z-TOAC-OH and Fmoc-TOAC-OH were characterized by X-ray diffraction. Details of these structures (in particular of the first 2-*alkoxy*-5(4*H*)-oxazolones ever solved by X-ray diffraction) will be published separately.

Syntheses of the N^{α}-protected Ala/TOAC peptide methyl esters and *tert*-butylamides with an N-terminal TOAC residue were achieved in anhydrous acetonitrile under reflux either by using the 5(4*H*)-oxazolones or the symmetrical anhydride mentioned above. Removal of the Fmoc N^{α}-protecting group was performed by treatment with a 10% diethylamine solution in acetonitrile. In addition, we confirmed results from earlier studies [12, 15, 16] that the acidic and the reducing conditions required to remove the Boc- and Z-groups, respectively, are not compatible with the full chemical integrity of the nitroxide moiety. Therefore, introduction of a TOAC residue at an *internal* position and subsequent elongation of the peptide chain were obtained using Fmoc N^{α}-protection. The Ala residues were incorporated using the symmetrical anhydride approach.

The physical properties of the hydantoin, the free amino-acid, and a number of amino acid derivatives and Ala/TOAC peptides to the pentamer level are listed in Table 1.

Crystal-state Conformational Analysis

The preferred conformation of the doubly spin-labelled, terminally blocked pentapeptide *p*BrBz-TOAC-(L-Ala)$_2$-TOAC-L-Ala-NH*t*Bu hemihydrate in the crystal state was assessed by X-ray diffraction. The molecular structure with the atomic numbering scheme is illustrated in Fig. 1. Fig. 2 shows a projection along the *z*-axis.

The succession of similar pairs of ϕ,ψ values [20] [average $(\phi,\psi) = (-61.3°, -38.1°)$] along the peptide chain generates a helical structure, which can be described as a right-handed 3_{10}-helix, reasonably close to the ideal case ($\phi,\psi = -57°, -30°$) [21]. The helical structure is stabilized by four successive intramolecular $1 \leftarrow 4$ C–O···H=N H-bonds of the C_{10} (β-turn)-III type [22, 23]. The range of observed N···O distances is 3.02–3.31 Å [24]. The deviation of the ω angles from the ideal value of the *trans* planar –CONH– unit (180°) is significant only for the C-terminal -L-Ala-NH*t*Bu amide bond ($\Delta\omega$=14.1°). The phenyl group of the *p*BrBz moiety is only slightly rotated from the plane of the N-terminal amide group [the N1–C1–C2–C3 torsion angle is −9.0 (20)°]. The torsion angles of the *tert*-butylamido group [−173.7(21), 54.8(25) and −66.3(25)°] indicate staggering of the three methyls about the C6A–N6 bond.

The N–O bond lengths of the nitroxide groups of the TOAC residues at positions 1 and 4 are 1.29(2) and 1.30(2) Å, respectively. Typical lengths for a

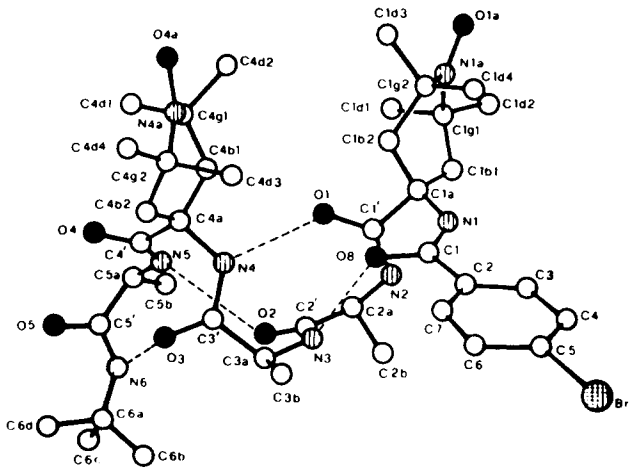

Fig. 1 X-ray diffraction structure of *p*BrBz-TOAC-(L-Ala)$_2$-TOAC-L-Ala-NH*t*Bu with numbering of the atoms. The intramolecular H-bonds are represented by dashed lines.

Table 1 Physical Properties for the TOAC Derivatives and Peptides

Compound	Melting point (°C)	Recryst. solvent[a]	$[\alpha]_D^{20}$ (°)[b]	TLC			VIS		IR[c]
				R_{F1}	R_{F2}	R_{F3}	λ_{max}	(ε)c	
TOAC hydantoin	>230	EtOH/H_2O	–	0.75	0.95	0.40	436	(5.8)	3160,1775, 1720
H-TOAC-OH	228–230	H_2O (pH 6)	–	0.00	0.60	0.00	430	(7.0)	3445, 3150, 1615
*p*BrBz-TOAC-OH	175–176	AcOEt	–	0.20	0.95	0.10	446 442	(10.5) (9.7)[d]	3360, 1738, 1704, 1661
Fmoc-TOAC-OH	165–166	AcOEt/PE	–	0.35	0.90	0.25	429	(5.5)	3342, 1722
Z-TOAC-OH	167–168	AcOEt/PE	–	0.25	0.90	0.20	435	(6.9)	3355, 1743, 1716
Boc-TOAC-OH	168–169	Et_2O/PE	–	0.65	0.90	0.25	433	(6.8)	3377, 1716
(Z-TOAC)$_2$O	129–130	AcOEt	–	0.95	–	0.35	448	(13.6)	3402, 1819, 1712
5(4*H*)-oxazolone from *p*BrBz-TOAC-OH	174–176	AcOEt/PE	–	0.95	–	0.85	451 422	(12.7) (10.1)[d]	1808, 1651
5(4*H*)-oxazolone from Fmoc-TOAC-OH	179–180	$CHCl_3$/PE	–	0.95	–	0.70	467	(9.9)	1831, 1682
5(4*H*)-oxazolone from Z-TOAC-OH	89–90	AcOEt	–	0.95	–	0.75	420	(8.8)	1819, 1692
5(4*H*)-oxazolone from Boc-TOAC-OH	114–115	AcOEt	–	0.85	–	0.60	469	(7.6)	1820, 1686
Z-TOAC-L-Ala-OMe	140–141	AcOEt/PE	–30.7	0.95	0.95	0.45	427	(7.6)	3276, 1720, 1663
Z-TOAC-(L-Ala)$_2$-OMe	71–73	AcOEt/PE	–24.5	0.85	0.95	0.35	431	(5.8)	3333, 1738, 1702, 1661
Fmoc-TOAC-L-Ala-N-H*t*Bu	141–143	AcOEt/PE	–3.6	0.70	0.95	0.40	429	(7.0)	3340, 1731, 1704, 1666
Z-TOAC-(L-Ala)$_2$-NH*t*-Bu	122–124	AcOEt/PE	+13.8	0.70	0.95	0.25	427	(7.2)	3535, 3302, 1699, 1658
Z-L-Ala-TOAC-L-Ala-NH*t*Bu	131–133	AcOEt/PE	–14.4	0.80	0.95	0.35	425	(7.0)	3343, 1682
Fmoc-L-Ala-TOAC-L-Ala-NH*t*Bu	133–135	AcOEt/PE	–27.0	0.90	0.95	0.35	425	(5.9)	3349, 1679
Fmoc-(L-Ala)$_2$-TOAC-L-Ala-NH*t*Bu	137–139	AcOEt/PE	–26.9	0.80	0.95	0.30	420	(11.9)	3341, 1662
*p*BrBz-TOAC-(L-Ala)$_2$-TOAC-L-Ala-NH*t*Bu	>230	AcOEt	54.0	0.50	0.90	0.10	447 422	(38.0) (31.2)[d]	3348, 1654
Boc-TOAC-(L-Ala)$_2$-T-OAC-L-Ala-NH*t*Bu	224–225	AcOEt/PE	32.8	0.70	0.90	0.25	420	(14.2)[d]	3381, 1661

[a] EtOH, ethyl alcohol; AcOEt, ethyl acetate; Et_2O, diethyl ether; PE, petroleum ether.
[b] c 0.5, methanol.
[c] λ_{max} (nm) and $\varepsilon(1 \times mol^{-1} \times cm^{-1})$; all VIS spectra were recorded in methanol, with the exception of those of the anhydride and the 5(4*H*)-oxazolones which were measured in ethyl acetate (for reasons of chemical stability of the compounds).
[d] Shoulder
[e] The IR spectra were obtained in KBr pellets (only bands in the 3600–3150 and 1900–1600 cm^{-1} regions are reported).

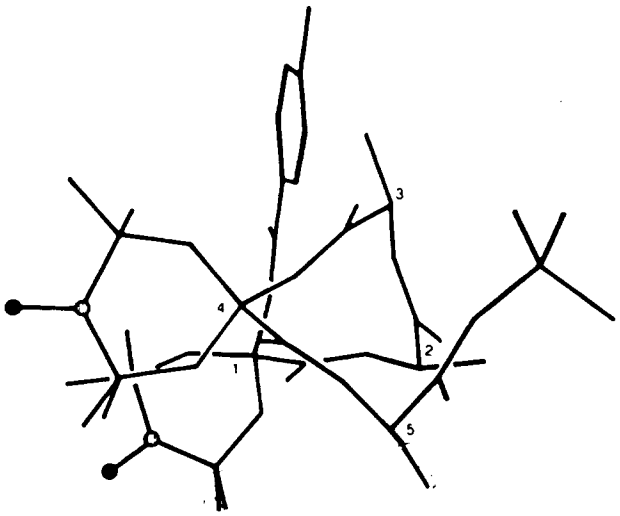

Fig. 2 Projection of the *p*BrBz-TOAC-(L-Ala)$_2$-TOAC-L-Ala-NH*t*Bu molecule down the *z*-axis (the helix axis). Position of a given amino acid in the peptide chain is indicated by a number on its C^{α} atom. The N and O atoms of the two nitroxide groups are represented by dashed and full circles, respectively. The almost perfect triangular shape of the 3_{10}-helix stands out clearly.

(sp^2)N–O single bond are longer (in the range 1.39–1.40 Å) [25, 26]. The values of the external O–N–C bond angles and the internal CG1–N–CG2 bond angle are found between 116–120(2)° and 124–125(1)°, respectively. The angle between the N–O bond and the CG1–N–CG2 plane is 1.4(17)° for residue 1 and 5.16(36)° for residue 4.

The two nitroxide groups are oriented roughly perpendicular to the helix axis and approximately parallel to each other. The dihedral angle between normals to the average planes of the two piperidinyl rings is 15.9° and the dihedral angle O4A–N4A ... N1A–O1A is −24.2(25)°. The distances between centres of the rings and between mid-points of the N–O bonds are 6.30 and 7.32 Å, respectively. Both hexatomic rings are found in a conformation close to the *twist-boat* disposition with the following puckering parameters: Q_T = 0.64(1) Å, ϕ_2 = 100(1)°, θ_2 = 90(1)° for TOAC^1, and Q_T = 0.60(2) Å, ϕ_2 = 91(2)°, θ_2 = 90(2)° for TOAC^2 [27].

Along the direction of the *z*-axis, the helical molecules of the pentapeptide hemihydrate are connected by head-to-tail H-bonding. The crystal packing mode is characterized by two intermolecular N–H ··· O–C H-bonds involving the N1–H and N2–H groups as donors and the O_4=C_4' and O_5=C_5' groups of a symmetry-related molecule (x, y, $1-z$) as acceptors, respectively. The N ··· O separations are 3.00–3.01 Å [24]. The co-crystallized water molecule is H-bonded as donor to the O5=C5′ amide carbonyl [28] of a symmetry-related molecule (x, y, $1-z$) and to the O4A–N4A nitroxide group [29] of a symmetry-related molecule ($3-x$, $1/2+y$, $3-z$). The O ··· O separations are 2.91 and 2.97 Å, respectively [30].

Solution Conformational Analysis

FTIR Absorption. The conformational preferences of the Ala/TOAC peptides in solution were first determined by FTIR absorption in the structure-supporting solvent $CDCl_3$ as a function of concentration (over the range 0.1–10 mM). Fig. 3 illustrates the FTIR absorption spectra (N–H stretching region) of the N^{α}-urethane, C-*tert*-butylamide series from the di- to the pentapeptide.

The curves are characterized by two bands at 3442–3427 cm^{-1} (free NH groups) and 3387–3335 cm^{-1} (H-bonded NH groups), respectively [5, 31]. The intensity of the low-frequency band relative to the high-frequency band (A_H/A_F ratio) significantly increases as main-chain length increases; concomitantly, the absorption maximum of the former band shifts markedly to lower wavenumbers. The band related to H-bonded NH groups is negligible in the dipeptide ester (not shown).

Using the Mizushima dilution method [32], we have been able to show that even at 10 mM concentration, self-association via N–H ··· O–C intermolecular H-bonding is of minor significance (less than 10%) for the tri- and tetrapeptides. Therefore, the observed H-bonding should be interpreted as arising almost exclusively from intramolecular N–H ··· O=C interactions. However, in the case of the pentapeptides, self-association plays a significant role, particularly at concentrations >1 mM. In any event, even at 0.1 mM concentration the intensity of the band related to H-bonded NH groups is remarkably high, suggesting the occurrence of large populations of intramolecularly H-bonded species.

The present FTIR absorption investigation has provided convincing evidence that main-chain length-dependent intramolecular H-bonding is an important factor for the terminally blocked Ala/TOAC peptides in $CDCl_3$ solution. The observation

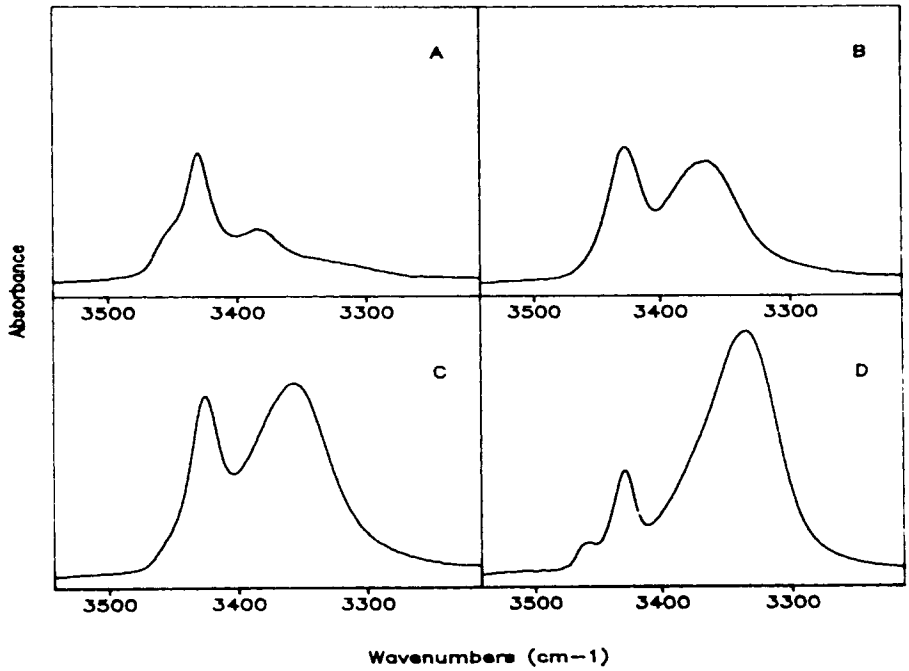

Fig. 3 FTIR absorption spectra in the 3500–3250 cm^{-1} region of Fmoc-TOAC-L-Ala-NH*t*Bu (A), Fmoc-L-Ala-TOAC-L-Ala-NH*t*Bu (B), Fmoc-(L-Ala)$_2$-TOAC-L-Ala-NH*t*Bu (C) and Boc-TOAC-(L-Ala)$_2$-TOAC-L-Ala-NH*t*Bu (D) in $CDCl_3$ solution (concentration 10 mM).

of the 3387–3335 cm^{-1} band in the di-, tri-, tetra- and pentapeptide amides, which is negligible in the dipeptide ester, seems to indicate that the Ala/TOAC peptides do not tend to assume a γ-turn form [23, 33], even in a solvent of low polarity, and highlights the propensity of the tripeptide to adopt a β-turn conformation [22, 23] which may evolve in a series of consecutive β-turns (3_{10}-helices) [21] in longer peptides.

Circular Dichroism. In the VIS region of the absorption spectrum nitroxide-containing compounds show a very weak (ε = 5–15), solvent-dependent n–π^* band at 400–500 nm [8, 34, 35]. In the Ala/TOAC peptides synthesized in this work this band is visible at 420–447 nm in MeOH solution (Table 1).

The preferred conformation of the *p*BrBz-TOAC-(L-Ala)$_2$-TOAC-L-Ala-NH*t*Bu pentapeptide in solution was examined in detail using CD spectroscopy. In the VIS region a relatively strong, positive Cotton effect is seen at 423 nm in MeOH (Figure 4). The intensity of this CD band decreases significantly by changing solvent (MeOH $\cong$ EtOH > $CHCl_3$ > TFE > DMSO > HFIP). A 25% reduction in ellipticity is produced also by heating the methanol solution from −5 to 40°C. A strictly parallel phenomenon is exhibited by the doubly labelled Boc-protected pentapeptide analogue. However, a 20–70 fold weaker Cotton effect is observed in this region in the CD spectra of the singly labelled L-Ala/TOAC di-, tri- and tetrapeptides.

Fig. 5 illustrates the CD pattern of the Nα-*para*-bromobenzoylated pentapeptide in the 210–300 nm region in four different alcohols. This spectral region is dominated by the contribution of the *para*-bromobenzamido chromophore, the absorption maximum of which is centred near 240 nm [36]. This conclusion is corroborated by the observation that this characteristically exciton split curve is absent in the CD spectrum of the Boc-protected pentapeptide analogue. The Cotton effect at higher wavelengths (250–255 nm) is *positive*, while that at lower wavelengths (229–231 nm) is *negative*, suggesting that an interaction is operative between the N-terminal *para*-bromobenzamido chromophore and the amido chromophores of the peptide chain arranged in a *right*-handed 3_{10}-*helical* array [36]. The strength of the two oppositely signed CD bands decreases in the order: MeOH $\cong$ EtOH > TFE > HFIP.

From these results we are inclined to conclude that the intensity of the CD band near 425 nm and those of the exciton split bands centred near 240 nm

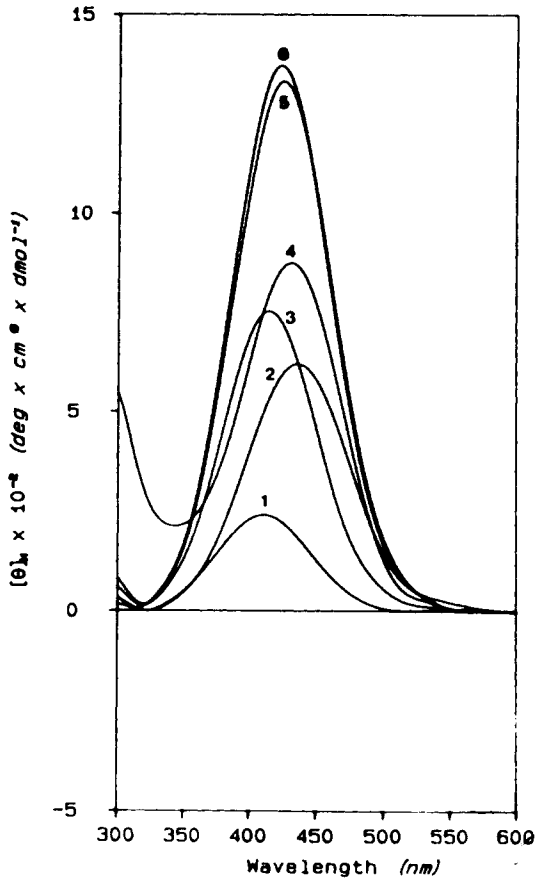

Fig. 4 Circular dichroism spectra in the 300–600 nm region of *p*BrBz-TOAC-(L-Ala)$_2$-TOAC-L-Ala-NH*t*Bu in HFIP (1), DMSO (2), TFE (3), $CHCl_3$ (4), EtOH (5) and MeOH (6) (concentration 2 mM).

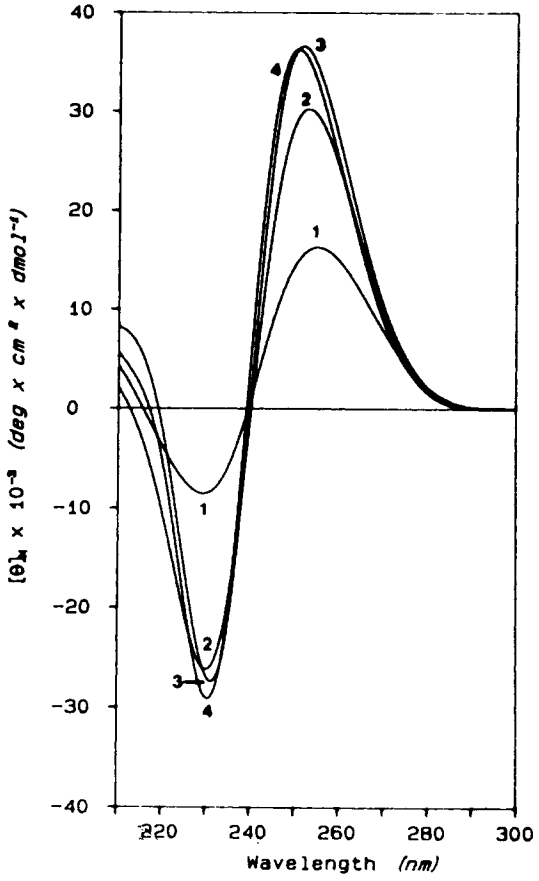

Fig. 5 Circular dichroism spectra in the 210–300 nm region of *p*BrBz-TOAC-(L-Ala)$_2$-TOAC-L-Ala-NH*t*Bu in HFIP (1), TFE (2), EtOH (3) and MeOH (4) (concentration 1 mM).

represent excellent probes for the determination of the population of 3_{10}-helical species in the conformational equilibrium mixtures of *p*BrBz-TOAC-(L-Ala)$_2$-TOAC-L-Ala-NH*t*Bu under different experimental conditions. In this connection it is interesting to note that the following rank orders of structure-supporting solvents may be established: (i) MeOH $\cong$ EtOH > TFE > HFIP (for the hydroxylated solvents), and (ii) $CHCl_3$ > DMSO (for the non-hydroxylated solvents).

Cyclic Voltammetry. This electrochemical technique revealed that in EtOH both the singly labelled reference compound *p*BrBz-TOAC-OH and the doubly labelled pentapeptide *p*BrBz-TOAC-(L-Ala)$_2$-TOAC-L-Ala-NH*t*Bu undergo an uncomplicated, reversible nitroxide-based oxidation centred at $E_{1/2}$ = 0.324 and 0.315 V, as mean values of the potentials for anodic and cathodic peak currents, respectively (Figure 6). For the amino acid derivative the voltammetric profile is that anticipated for a simple one-electron reversible charge transfer by most of the criteria of stationary electrode polarography [37], i.e. the ratio of the cathodic to anodic peak currents, i_p^c/i_p^a, is unity over the range of the experimental (20–200 mV s^{-1}) cyclic scan rate, and the peak-to-peak separation, ΔE_p, and the peak width, $E_p - E_{p/2}$, are 65 and 59 mV (60 and 57 mV for ferrocene), respectively.

For the pentapeptide the height of the oxidation wave is approximately double that of the wave displayed by the reference compound under identical experimental conditions, thereby implying a two-electron step. In addition, an inspection of the shape

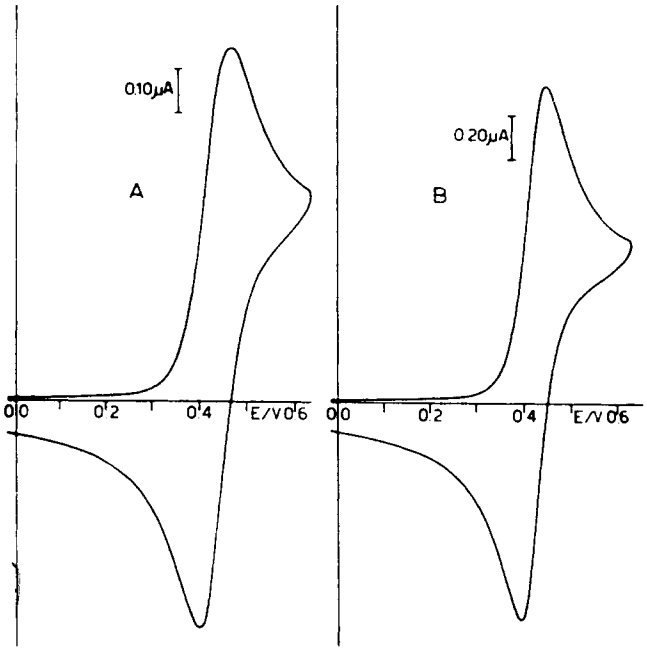

Fig. 6 Cyclic voltammogram for oxidation of 1.56 mM *p*BrBz-TOAC-OH (A) and 1.30 mM *p*BrBz-TOAC-(L-Ala)$_2$-TOAC-L-Ala-NH*t*Bu (B) in EtOH solution, 0.2 M $NaClO_4$, at 25° (scan rate 0.2 V s^{-1}).

of the voltammetric response indicates that it is slightly sharper than that predicted for a single-stepped two-electron charge transfer reaction involving two non-interacting redox sites in the same molecule under a merely statistical control: ΔE_p and $E_p - E_{p/2}$ are 50 and 45 mV rather than 58.5 and 57 mV as expected [38, 39]. This finding is attributed to a small difference between the E^o values for the two individual one-electron transfers (E_1^0 = 0.311 V; E_2^0 = 0.323 V) [39] and suggests a weak electronic interaction between the redox sites, but, most remarkably, it reveals that electrons are exchanged almost in a single shot. These observations embody the important structural implication that a simultaneous approach of both nitroxide sites to the electrode surface is not precluded. This conclusion, in turn, strongly supports the view that the 3_{10}-helical conformation observed in the crystal state for the pentapeptide (with the two nitroxide groups located on the same side of the helix) is largely preserved in EtOH solution.

Electron Spin Resonance. The aim of this ESR study was to correlate the secondary structure of the pentapeptide *p*BrBz-TOAC-(L-Ala)$_2$-TOAC-L-Ala-NH*t*Bu in various alcohols. ESR spectra of a doubly labelled (biradical) peptide provide a measure of the amount of *J*-coupling between the nitroxide spins [40, 41]. *J*-coupling increases with decreasing distance between the spins. The shape of the ESR spectra of a nitroxide biradical in solution depends on the relative values of *J* and the isotropic hyperfine coupling a_N of the nitroxide nitrogen nuclei. In the weak coupling regime ($J \ll a_N$) ESR spectra are characterized by three nitrogen hyperfine lines, as it occurs for a monoradical species. The lines broaden for increasing *J*. Strong coupling ($J \gg a_N$), however, gives spectra with five lines (which are referred to as transitions 1 through 5) with an intensity ratio 1:2:3:2:1 and separated by $a_N/2$ [42]. In the intermediate case $J \cong a_N$ the line intensities deviate from the above ratios. The spin labels in the pentapeptide are separated by $i \rightarrow i + 3$ spacing and it is expected that strong coupling will result if the peptide adopts a 3_{10}-helix conformation. Thus, the amount of helicity can be correlated to the amount of *J*-coupling observed in the ESR spectra.

Spectra for the pentapeptide in four alcohols of different polarity at room temperature are shown in Fig. 7. On the basis of the reasoning above, it appears that amount of helicity follows the order MeOH > EtOH > TFE ≅ HFIP, with MeOH giving the strongest five-line pattern.

However, we note that in MeOH the second and fourth lines are selectively broadened. Such broadening, which is even more pronounced in EtOH, is characteristic for flexible biradicals [43] and suggests that the pentapeptide is flickering in and out of the helical conformation. This motion modulates the *J* interaction which contributes an additional term to the width of the second and fourth lines of the spectrum and to two components of the triple degenerate central line.

Assuming a simple model where the interaction occurs only in the helix conformation and indicating by $\bar{J}$ the mean value of *J*, the linewidth contribution is:

$$T_2^{-1} = \frac{a_N^2}{4J^2} j(\bar{J})$$

The spectral density $j(\bar{J})$ depends on *J* and on the dynamics of the flickering motion, being proportional to the inverse of the modulation frequency, i.e. to the lifetime τ of the unordered and helical conformations [42–44]. It should be noted that in the case of extreme broadening the second and fourth lines disappear and strong exchange can appear as weak exchange

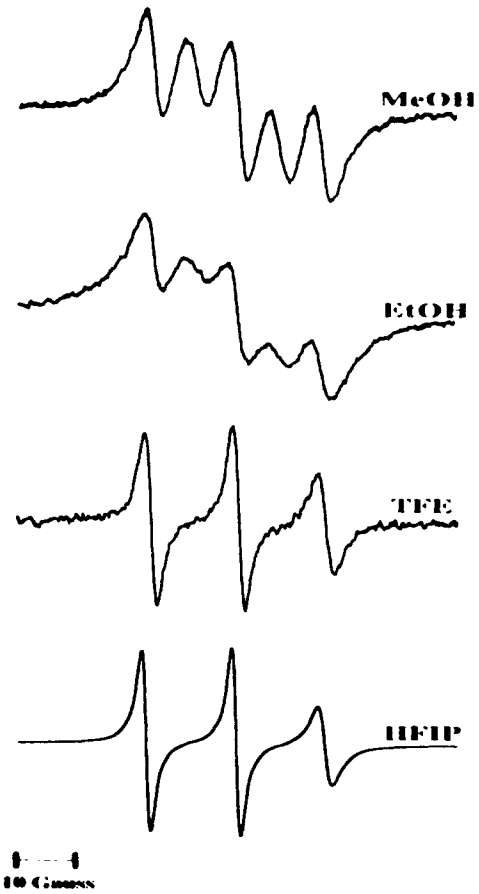

Fig. 7 ESR spectra of *p*BrBz-TOAC-(L-Ala)$_2$-TOAC-L-Ala-NH*t*Bu in the denoted neat alcohols at room temperature. Concentrations for the samples are: 0.98 mM in MeOH; 1.96 mM in EtOH; 0.039 mM in TFE; 4.0 mM in HFIP (the sample in TFE was kept at low concentration to avoid peptide aggregation).

[45]. Spectral integration allows for the separation of these two extreme cases and we have determined that the HFIP and TFE spectra are indeed weakly coupled. Thus, the pentapeptide is largely unfolded in these solvents.

The dynamics of the flickering process is expected to be influenced by the temperature. Fig. 8 shows how the broadening of the second and fourth lines of the peptide in MeOH increases by lowering the temperature. The spectral changes reflect the temperature dependence of the ratio $j(\bar{J})/\bar{J}^2$ and this effect could be caused either by an increase of τ or by a decrease of J (i.e. by a reduced helical content). The latter situation would contrast with the results of the CD reported above and with the general observation that peptide helical content in alcohols tends to

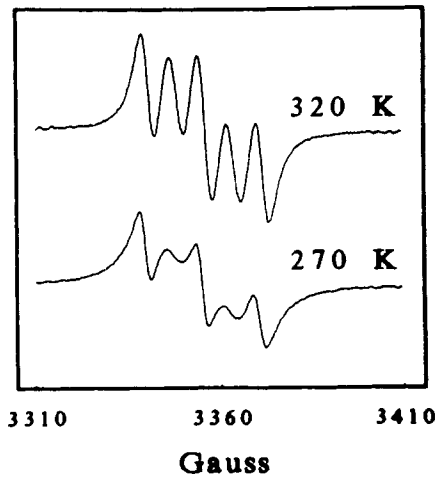

Fig. 8 ESR spectra of *p*BrBz-TOAC-(L-Ala)$_2$-TOAC-L-Ala-NH*t*Bu in MeOH as a function of temperature (concentration 1 mM).

increase as the temperature is lowered. Therefore, we are inclined to attribute the broadening of the ESR lines at low temperature to the slowing down of the flickering process.

Biradical J-coupling can arise from both through bond and through space overlap of the electron wave functions. Of course, only the through space contribution provides information on peptide conformation. The TOAC nitroxide is closer to the peptide backbone than other previously used peptide spin labels [40, 41] and this results in fewer σ-bonds between the spins and the possibility of a significant through bond contribution. Recent experiments with transient biradicals have determined the relationship between the number of σ-bonds and the resulting J-coupling [46]. Using their parameters we calculate the through bond contribution to be 0.23 gauss, which is less than the intrinsic linewidth of a nitroxide monoradical. The results described here with TFE and HFIP show little J-coupling and this could not occur if there were a significant through bond contribution.

DISCUSSION

A series of L-Ala-based oligopeptides (to the pentamer level) containing one or two TOAC residues were synthesized in solution using the 5(4*H*)-oxazolone or the symmetrical anhydride method. Introduction of a

TOAC residue at an internal position and subsequent elongation of the peptide chain requires Fmoc N^{α}-protection [16]. Analytical characterization of the various compounds was achieved by melting point determination, thin-layer chromatography in two or three different solvent systems, polarimetry, UV–VIS and IR spectroscopies (the latter in the solid state).

An X-ray diffraction investigation revealed that the terminally blocked, doubly labelled pentapeptide with the sequence -TOAC-$(Ala)_2$-TOAC-Ala- adopts a 3_{10}-helical structure in the crystal state. The right-handed screw sense of the helix is dictated by the L-configuration of the internal Ala residues. The two nitroxide groups protrude outwards of the peptide scaffold, separated by one turn of the helical structure, i.e. by approximately 6.5–7.0 Å.

Combined FTIR absorption, CD, cyclic voltammetry and ESR measurements provide convincing evidence that the right-handed 3_{10}-helical conformation of the pentapeptide is essentially preserved in structure-supporting solvents, such as MeOH, EtOH and $CHCl_3$. The amount of helical structure tends to decrease substantially as the polarity of the solvent (TFE, DMSO, HFIP) increases. The results obtained from these techniques, taken together, also suggest that an interaction is operative between the two nitroxide labels located on the same side of the helical structure.

Recently, MD calculations were performed on the peptide Ac-(L-Ala)$_3$-NHMe in various alcohols and alcohol/water mixtures [47]. Free energy curves were determined for α-helical and extended conformations. Although the 3_{10}-helical conformation was not considered, these calculations still provide a prediction on the relative helix-forming properties of the various solvents. The MD calculations indicated that MeOH is a stronger helix former than TFE and this is consistent with the present results. The other alcohols were not examined in the MD study. However, we have explored the ESR spectra for the pentapeptide in alcohol/water mixtures (data not shown) and thus far there is excellent agreement with the MD calculations. The experiments reported here are among the first to systematically probe the amount of helix structure of short peptides in various solvents, and the apparent agreement with recent theory is extremely encouraging.

In summary, the conformational data described in this paper unambiguously indicate that the TOAC residue has a marked intrinsic tendency to adopt φ,ψ backbone torsion angles in the helical region of the conformational map [48], in analogy to many other $C^{\alpha,\alpha}$-disubstituted glycines such as the prototype Aib and the cycloaliphatic analogue Ac_6c [1–5]. This main-chain structural property, coupled with the presence of the nitroxide group characterizing the lateral chain, makes TOAC an excellent probe for exploring β-bends and $3_{10}/\alpha$-helices in peptides doubly labelled at appropriate relative positions.

Acknowledgement

This research was supported in part by a V.J.H. grant (G.M. 46870) to G.L.M.

REFERENCES

1. C. Toniolo and E. Benedetti (1991). Structures of polypeptides from α-amino acids disubstituted at the α-carbon. *Macromolecules 24*, 4004–4009.
2. C. Toniolo (1993). $C^{\alpha,\alpha}$-symmetrically disubstituted glycines: useful building blocks in the design of conformationally restricted peptides. *Janssen Chim. Acta 11*, 10–16.
3. P. K. C. Paul, M. Sukumar, R. Bardi, A. M. Piazzesi, G. Valle, C. Toniolo and P. Balaram (1986). Stereochemically constrained peptides. Theoretical and experimental studies on the conformations of peptides containing 1-aminocyclohexanecarboxylic acid. *J. Am. Chem. Soc. 108*, 6363–6370.
4. V. Pavone, E. Benedetti, V. Barone, B. Di Blasio, F. Lelj, C. Pedone, A. Santini, M. Crisma, G. M. Bonora and C. Toniolo (1988). Structural versatility of peptides from $C^{\alpha,\alpha}$-dialkylated glycines. A conformational energy computation and X-ray diffraction study of homopeptides from 1-aminocyclohexane-1-carboxylic acid. *Macromolecules 21*, 2064–2070.
5. M. Crisma, G. M. Bonora, C. Toniolo, A. Bavoso, E. Benedetti, B. Di Blasio, V. Pavone and C. Pedone (1988). Structural versatility of peptides from $C^{\alpha,\alpha}$-dialkylated glycines. An infrared absorption and ^1H nuclear magnetic resonance study of homopeptides from 1-aminocyclohexane-1-carboxylic acid. *Macromolecules 21*, 2071–2074.
6. S. M. Miick, G. V. Martinez, W. R. Fiori, A. P. Todd and G. L. Millhauser (1992). Short alanine-based peptides may form 3_{10}-helices and not α-helices in aqueous solution. *Nature 359*, 653–655.
7. G. L. Millhauser (1992). Selective placement of electron spin resonance spin labels: new structural methods for peptides and proteins. *TIBS 17*, 448–452.
8. O. H. Griffith and A. S. Waggoner (1969). Nitroxide free radicals: spin labels for probing biomolecular structure. *Acc. Chem. Res. 2*, 17–24.

9. H. Iwamura and N. Koga (1993). Studies of organic di-, oligo-, and polyradicals by means of their bulk magnetic properties. *Acc. Chem. Res. 26*, 346–351.
10. C. Degrand, B. Limoges and R. L. Blankespoor (1993). Synthesis of nitroxides for use as procationic labels and their incorporation into Nafion films. *J. Org. Chem. 58*, 2573–2577.
11. C. L. Nakaie, G. Goissis, S. Schreier and A. C. M. Paiva (1981). pH dependence of EPR spectra of nitroxides containing ionizable groups. *Braz. J. Med. Biol. Res. 14*, 173–180.
12. C. R. Nakaie, S. Schreier and A. C. M. Paiva (1983). Synthesis and properties of spin-labeled angiotensin derivatives. *Biochim. Biophys. Acta 742*, 63–71.
13. R. Seidemann and L. Dulog (1986). *N*-carboxyanhydride of 4-amino-4-carboxy-2,2,6,6-tetramethylpiperidine-1-oxyl, a new paramagnetic monomer. *Makromol. Chem. 187*, 2545–2551.
14. R. Seidemann (1989). Synthesis and oligomerization of a paramagnetic monomer. *Makromol. Chem. 190*, 1891–1902.
15. L. Dulog and W. Wang (1992). A bisnitroxyl dipeptide. *Liebigs Ann. Chem.*, 301–303.
16. R. Marchetto, S. Schreier and C. R. Nakaie (1993). A novel spin-labeled amino acid derivative for use in peptide synthesis. (9-Fluorenylmethyloxycarbonyl)-2,2,6,6-tetramethylpiperidine-*N*-oxyl-4-amino-4-carboxylic acid. *J. Am. Chem. Soc. 115*, 11042–11043.
17. G. M. Sheldrick (1986). SHELX 86. Program for the solution of crystal structures. University of Göttingen, Germany.
18. G. M. Sheldrick (1994). *J. Appl. Crystallogr.*, in press.
19. A. Rassat and P. Rey (1967). Nitroxides. XXIII. Préparation d'aminoacides radicalaires et de leurs sels complexes. *Bull. Soc. Chim. Fr.*, 815–817.
20. IUPAC-IUB Commission on Biochemical Nomenclature (1970). Abbreviations and symbols for the description of the conformation of polypeptide chains. *Biochemistry 9*, 3471–3479.
21. C. Toniolo and E. Benedetti (1991). The polypeptide 3_{10}-helix. *TIBS 16*, 350–353.
22. C. M. Venkatachalam (1968). Stereochemical criteria for polypeptides and proteins. V. Conformation of a system of three-linked peptide units. *Biopolymers 6*, 1425–1436.
23. C. Toniolo (1980). Intramolecularly hydrogen-bonded peptide conformations. *C.R.C. Crit. Rev. Biochem. 9*, 1–44.
24. C. H. Görbitz (1989). Hydrogen-bond distances and angles in the structures of amino acids and peptides. *Acta Crystallogr. B45*, 390–395.
25. F. H. Allen, O. Kennard, D. G. Watson, L. Brammer, A. G. Orpen and R. Taylor (1987). Tables of bond lengths determined by X-ray and neutron diffraction. Part 1. Bond lengths in organic compounds. *J. Chem. Soc., Perkin Trans. 2* S1–S19.
26. J. Lajzerowicz-Bonneteau in: *Spin Labelling. Theory and Applications*, L. J. Berliner, Ed., p. 239–249, Academic Press, New York 1976.
27. D. Cremer and J. A. Pople (1975). A general definition of ring puckering coordinates. *J. Am. Chem. Soc. 97*, 1354–1358.
28. C. H. Yang, J. N. Brown and K. D. Kopple (1979). Peptide–water association in peptide crystals. *Int. J. Pept. Protein Res. 14*, 12–20.
29. C. Gilon, S. Cohen and Y. Siderer (1986). The crystal structure of the photosynthetic inhibitors DCMU and DTPU. *Biopolymers 25*, 1615–1621.
30. J. Mitra and C. Ramakrishnan (1977). Analysis of O–H ··· O hydrogen bonds. *Int. J. Pept. Protein Res. 9*, 27–48.
31. D. F. Kennedy, M. Crisma, C. Toniolo and D. Chapman (1991). Studies of peptides forming 3_{10}- and α-helices and β-bend ribbon structures in organic solution and in model membranes by Fourier transform infrared spectroscopy. *Biochemistry 30*, 6541–6548.
32. A. Mizushima, T. Shimanouchi, M. Tsuboi and R. Souda (1952). Additional studies of the intramolecular hydrogen bonding in acetylglycine *N*-methylamide. *J. Am. Chem. Soc. 74*, 270–271.
33. G. Némethy and M. P. Printz (1972). The γ-turn, a possible folded conformation of the polypeptide chain. Comparison with the β-turn. *Macromolecules 5*, 755–758.
34. R. Briére, H. Lemaire and A. Rassat (1965). Nitroxides. XV. Synthèse et études des radicaux libres stables pipéridiniques et pyrrolidiniques. *Bull. Soc. Chim. Fr.*, 3273–3283.
35. T. Kawamura, S. Matsunami and T. Yonezawa (1967). Solvent effects on the *g*-value of di-*t*-butyl nitric oxide. *Bull. Chem. Soc. Jpn 40*, 1111–1115.
36. C. Toniolo, F. Formaggio, M. Crisma, H. E. Schoemaker and J. Kamphuis (1994). The *p*-bromobenzamido chromophore as a circular dichroic probe for the assignment of the screw sense of helical peptides. *Tetrahedron: Asymmetry 5*, 507-510.
37. R. S. Nicholson and I. Shain (1964). Theory of stationary electrode polarography. Single scan and cyclic methods applied to reversible, irreversible and kinetic systems. *Anal. Chem. 36*, 706–723.
38. J. B. Flanagan, S. Margel, A. J. Bard and F. C. Anson (1978). Electron transfer to and from molecules containing multiple, noninteracting redox centers. Electrochemical oxidation of poly (vinylferrocene). *J. Am. Chem. Soc. 100*, 4248–4253.
39. D. E. Richardson and H. Taube (1981). Determination of E_2^0–E_1^0 in multistep charge transfer by stationary-electrode pulse and cyclic voltammetry: application to binuclear ruthenium ammines. *Inorg. Chem. 20*, 1278–1285.

40. S. M. Miick, G. V. Martinez, W. R. Fiori, A. P. Todd and G. L. Millhauser (1992). Short alanine-based peptides may form 310-helices and not α-helices in aqueous solution. *Nature 359*, 653–655.
41. W. R. Fiori, S. M. Miick and G. L. Millhauser (1993). Increasing sequence length favors α-helix over 3_{10}-helix in alanine-based peptides: evidence for a length dependent structural transition. *Biochemistry 32*, 11957–11962.
42. G. R. Luckhurst in: *Spin Labelling. Theory and Applications*, L. J. Berliner, Ed., p. 133–181, Academic Press, New York 1976.
43. G. R. Luckhurst (1966). Alternating linewidths. A novel relaxation process in the electron resonance of biradicals. *Mol. Phys. 10*, 543–550.
44. V. N. Parmon and G. M. Zhidomirov (1974). Calculation of the ESR spectrum shape of the dynamic biradical system. *Mol. Phys. 27*, 367–375.
45. H. Lemaire, A. Rassat, P. Rey and G. R. Luckhurst (1968). Le téréphthalate de di(tétraméthyl-2,2,6,6-pipéridinyl-4-oxyle-1) est-il un biradical á échange fort ou à échange faible? *Mol. Phys. 14*, 441–447.
46. G. L. Closs, M. D. E. Forbes and P. Piotrowiak (1992). Spin and reaction dynamics in flexible polymethylene biradicals as studied by EPR, NMR and optical spectroscopy and magnetic field effects. Measurements and mechanisms of scalar electron spin–spin coupling. *J. Am. Chem. Soc. 114*, 3285–3294.
47. C. L. Brooks, III and L. Nilsson (1993). Promotion of helix formation in peptides dissolved in alcohol and water–alcohol mixtures. *J. Am. Chem. Soc. 115*, 11034–11035.
48. S. S. Zimmerman, M. S. Pottle, G. Némethy and H. A. Scheraga (1977). Conformational analysis of the 20 naturally occurring amino acid residues using ECEPP. *Macromolecules 10*, 1–9.